



CHORUS

This is the accepted manuscript made available via CHORUS. The article has been published as:

Two-potential approach to pair creation from the vacuum

Q. Z. Lv, Y. T. Li, Q. Su, and R. Grobe

Phys. Rev. A **95**, 022128 — Published 27 February 2017

DOI: [10.1103/PhysRevA.95.022128](https://doi.org/10.1103/PhysRevA.95.022128)

Two-potential approach to the pair creation from the vacuum

Q.Z. Lv^{1,2}, Y.T. Li¹, Q. Su^{1,2} and R. Grobe²

(1) Beijing National Laboratory for Condensed Matter Physics, Institute of Physics,
Chinese Academy of Sciences, Beijing 100190, China

(2) Intense Laser Physics Theory Unit
and Department of Physics
Illinois State University, Normal, IL 61790-4560 USA

By applying a Foldy-Wouthysen-like transformation and a low momentum approximation to the usual quantum field theoretical Dirac Hamiltonian in one spatial dimension, we introduce a new Hamiltonian for which the kinetic portion and the original potential are diagonal in the corresponding spinor space and a second potential occurs that is off-diagonal. This two-potential Hamiltonian is applied to study the electron-positron pair creation process from the vacuum. Here the diagonal potential provides only the energy degeneracy of the lower and upper manifold of continuum states, which is one requirement for the permanent creation of particles. The off-diagonal potential actually triggers the creation process by providing the necessary coupling between the degenerate states. It also provides a concrete example of a model system for pair creation where the creation rate is perturbative in the coupling strength.

1. Introduction

It has been predicted that a sufficiently strong electric field can break down the electromagnetic vacuum and create electron-positron pairs. While an exciting new series of experiments is being planned in numerous laboratories [1-3] that try to exploit highly focused laser pulses to establish the required supercritical field situation, a direct experimental verification of the Schwinger pair creation process is presently still lacking [4-6].

The theoretical analysis of this predicted process is also conceptually rather challenging. One of the many reasons for these difficulties is that the potential representing the external field plays a dual role for the pair creation process. On the one hand, it creates the electrons and positrons from the vacuum and on the other hand it facilitates their permanent separation by providing the force field that can accelerate the electrons and positrons in opposite directions. The latter step of vacating the pair creation zone such that further particles can be created is actually crucially important as those particles that cannot leave the creation zone would Pauli block [7-9] the continued pair creation. In fact, if this removal of particles from the interaction zone is disabled, it can even bring the creation process to a complete halt. This complete suppression of pair creation despite supercritical field conditions was demonstrated in numerical simulations where the external force field was modeled by a potential well [10].

From an energetic point of view this dual role of the external potential manifests itself in the upward shifting of the lower energy continuum to create an important degeneracy with the positive energy states and then to provide simultaneously the coupling between these degenerate continuum states. Another consequence of this dual role is the non-perturbative scaling of the pair creation rate as a function of the electric field in the famous Schwinger expression [11], where the inverse of the potential strength V_0 occurs in the negative exponent. This analytical expression cannot be expanded as a series in positive powers of V_0 .

The dual role leads also to a well-known conceptual difficulty to uniquely identify particles inside the interaction zone, which makes an early recognition and tracing of the particle dynamics very challenging. So far each theoretical analysis has defined what constitutes a real particle based on the projection on force-free energy eigenstates of the corresponding system. Due to the existence of the $2mc^2$ mass gap, these states permit us to unambiguously use the (free) energy as a criterion to distinguish between electrons and positrons. This energy-based distinction, however, becomes impossible, for supercritical electric fields where the states of the lower and upper

manifold overlap. It has therefore been impossible to uniquely identify particles inside the interaction zone and important physical quantities that characterize the creation process such as number of particles or their energy spectrum become unambiguous only once the particles have left the pair creation zone.

In this work we propose an approximate model Hamiltonian that permits us to distinguish for the first time between the dual role of the external field. Using a Foldy-Wouthuysen like transformation of the Dirac equation [12], we can generate a new Hamiltonian that contains two potential terms. The first one leads to the required energy degeneracy and also provides the force field for the separation, but it does not couple the degenerate states. The second potential provides this coupling and therefore is solely responsible for the creation of the particles. There are three interesting outcomes of this model. It provides a fully analytical expression for the pair creation rate for the special case of a supercritical potential step and suggests that the widely-used Hund rule [13-15], which equates the transmission coefficient directly to the pair creation rate, can be generalized. It also provides for the first time a concrete example of a model system for pair creation where the pair creation rate is actually perturbative in the coupling strength. By being able to project onto the dressed energy eigenstates of the diagonal part of the Hamiltonian we can also obtain some first insight into the particles inside the interaction zone. The data reveal that even under a constant electric field there are regions where particles cannot be generated, suggesting that the pair creation rate is not solely determined by the local strength of the electric field. This is consistent with the findings of numerous other works. For example, Dinu et al. [16] have studied the locally-constant field approximation based on the polarization operator, whose imaginary part is related to the pair creation rate. Gies and Torgrimsson [17] have examined the role of the electrostatic energy between virtual electrons and positrons on the relationship between the Schwinger effect and critical transitions. The role of highly energetic re-collisions between created particles was examined, for example, by a work by Kuchiev [18] and recently by Meuren et al [19] using a semi-classical analysis.

This work is structured as follows. In Section 2 we derive the new form of the Hamiltonian from the Dirac Hamiltonian. In Section 3 we compare its predictions for the pair creation process due a supercritical potential step with that of the Dirac equation. In Section 4 we examine spatial probability densities inside a supercritical pair creation zone. We summarize this work in Section 5 and conclude with a brief summary of possible future challenges that this work raises.

2. Derivation of the approximate two-potential (ATP) Hamiltonian

There are two aspects that characterize Dirac-equation based framework for describing the pair creation process. First, as the force free (kinematic) part of the Dirac Hamiltonian is not diagonal in spinor space, each spinor component is nonzero for any force-free eigenstates associated with both the positive and negative energy manifolds. Despite being diagonal in this representation the potential $V(x)$ couples different spinor components. Second, as outlined in the introduction, the potential (such as a supercritical barrier of height $V_0 > 2c^2$) plays a dual role by up shifting the negative energy states and then coupling the resulting energy degenerate continuum states with each other.

In one spatial dimension the Dirac Hamiltonian is given by [20]

$$H_D = c p \sigma_1 + c^2 \sigma_3 + V(x) \quad (2.1)$$

where c is the speed of light, σ_i are the 2×2 Pauli matrices and below we denote the unit matrix with σ_0 . Atomic units are used, where three fundamental constants [amount of the charge of the electron, its mass m , and Planck's constants \hbar] are all unity by definition. As a result, the speed of light is $c=137.036$ a.u.

In order to bring the force-free part of the Hamiltonian $c p \sigma_1 + c^2 \sigma_3$ into a form that is diagonal in spinor space, we apply the unitary Foldy-Wouthysen transformation [12,21] to it, based on the 2×2 matrix: $U_{FW} \equiv [e \sigma_3 + p \sigma_1]/(p^2 + e^2)^{1/2}$ with the abbreviation $e \equiv c + (c^2 + p^2)^{1/2}$. The inverse of U_{FW} is identical to itself. We obtain $U_{FW} H_D U_{FW} = (c^4 + c^2 p^2)^{1/2} \sigma_3 + U_{FW} V(x) U_{FW}$. The transformed Hamiltonian $H_{TP} \equiv U_{FW} H_D U_{FW}$ contains two new potentials F_{diag} and F_{off} each of which is a complicated function of the original potential $V(x)$ and its higher order derivatives.

$$H_{TP} = (c^4 + c^2 p^2)^{1/2} \sigma_3 + F_{diag} \sigma_0 + i F_{off} \sigma_2 \quad (2.2a)$$

where

$$F_{diag} = e/(p^2 + e^2)^{1/2} V e/(p^2 + e^2)^{1/2} + p/(p^2 + e^2)^{1/2} V p/(p^2 + e^2)^{1/2} \quad (2.2b)$$

$$F_{\text{off}} = e/(p^2 + e^2)^{1/2} V p/(p^2 + e^2)^{1/2} - p/(p^2 + e^2)^{1/2} V e/(p^2 + e^2)^{1/2} \quad (2.2c)$$

While the kinetic portion is now in the desired diagonal form, the action of the complicated functions of the momentum operator on the potential $V(x)$ is very difficult. The diagonal part $F_{\text{diag}} \sigma_0$ describes the structure of that part of the external force that is solely responsible for dressing the created particles, while the off-diagonal term $i F_{\text{diag}} \sigma_2$ couples the states of the upper and lower energetic manifolds.

If we formally assume that the momentum operator p acts only on states with small velocities, we can Taylor expand the matrix U_{FW} up to first order in p/c , which simplifies the matrix operator to $U_{\text{FW}} = \sigma_3 + p/(2c) \sigma_1 + O[(p/c)^2]$, which is identical to its inverse (in the same order). This simplifies the action of U_{FW} on $V(x)$ significantly and we obtain $U_{\text{FW}} V(x) U_{\text{FW}} \approx [\sigma_3 + p/(2c) \sigma_1] V(x) [\sigma_3 + p/(2c) \sigma_1] + O[(p/c)^2]$. Using the commutator relationship $pV = -i dV/dx + Vp$, $\sigma_1 \sigma_3 = -i \sigma_2$ and $\sigma_1 \sigma_3 + \sigma_3 \sigma_1 = 0$, this expression simplifies to $U_{\text{FW}} V(x) U_{\text{FW}} \approx V(x) \sigma_0 - (2c)^{-1} dV/dx \sigma_2$. As a last step, we apply another unitary transformation based on $U_G = ((1, 0), (0, i))$ on both sides, and using $U_G \sigma_2 U_G^{-1} = -\sigma_1$ we obtain the final result of this derivation

$$U_G U_{\text{FW}} V(x) U_{\text{FW}} U_G^{-1} \approx H_{\text{ATP}} = (p^2/2 + c^2) \sigma_3 + V(x) \sigma_0 + (2c)^{-1} dV/dx \sigma_1 \quad (2.3)$$

We would like to point out that this is not a fully non-relativistic theory the kinetic part of the Hamiltonian still contains c as a finite parameter. This is important such that a finite mass gap $2mc^2$ can be maintained, permitting a clean separation of the dressing and transition triggering roles of the diagonal and off-diagonal parts of the potential. Furthermore, if the mass gap became infinitely wide, there would be no pair creation.

We will argue below, that this new approximate two-potential (ATP) Hamiltonian has the potential to make a direct analysis of the pair creation zone in terms of electrons and positrons possible. It will permit us to compute unambiguous spatial densities of electrons in this zone, while it captures the essential mechanisms of pair creation in a more transparent way. It has two major advantages over the traditional Dirac equation based theory. Its force-free part is diagonal in spinor space and it permits us to separate between a diagonal potential $V(x)$ (that causes the

degeneracy between the lower and upper energy manifolds) and a new force-based term proportional to $dV(x)/dx$ whose sole purpose is to trigger the pair creation process.

In order to establish that this model is reasonable we compare the pair creation rate obtained from this approach with that of the Dirac equation in Section 3. This comparison can be done on a fully analytical level for both approaches, if we use a simple barrier step potential. Here it is important to note that as long as $V(x)$ is sufficiently large to cause the required degeneracy ($V_0 > 2c^2$) even an infinitesimal force strength λ would be sufficient to cause a permanent creation of electron-positron pairs.

3. Analytical solution for the pair creation rate for a potential step

The quantum field theoretical problem of computing the number of created particles as a function of time can be mapped onto a quantum mechanical problem, where each single-particle state (representing the entire initially occupied Dirac sea) needs to be evolved in time [20]. We denote the corresponding force-free eigenstates of $H_0 = (c \sigma_1 p + \sigma_3 c^2)$ as $H_0 |u;E\rangle = E |u;E\rangle$ and $H_0 |d;E\rangle = -E |d;E\rangle$. Based on these field-free states the number of particles at a given energy $E = (c^4 + c^2 p^2)^{1/2}$ is usually defined by projecting all time-evolved states of the lower energy continuum on the electronic state $|u;E\rangle$ as $N(E;t) \equiv \int dE' |\langle u;E | \exp(-i H t) |d;E'\rangle|^2$. The time-derivative of its long-time limit is then used to define the pair creation rate at this energy, $\Gamma(E) \equiv dN(E;t)/dt$. We will show in Sec 3.2 how this rate can be obtained analytically from the corresponding transmission coefficient.

3.1 The transmission coefficient

We apply here the ATP Hamiltonian approach to examine the permanent pair creation process induced by a supercritical potential step $V(x) = V_0 \theta(x)$, where $\theta(x)$ is the unit-step function. For this system it is possible to use the ATP Hamiltonian to derive a fully analytical expression for the energy spectrum as well as the asymptotic long-time pair creation rate from the quantum mechanical transmission coefficient.

The ATP Hamiltonian for this external field configuration is given by

$$H_{ATP} = (c^2 + p^2/2) \sigma_3 + V_0 \theta(x) \sigma_0 + \lambda \delta(x) \sigma_1 \quad (3.1)$$

where we have introduced the coupling parameter λ to separate between the effects due to the dressing (associated with the diagonal potential) and the actual creation of the particles with strength λ .

In order to compute the required time evolution of the states $|d;E'\rangle$, it is advantageous to determine first the energy eigenstates of the ATP Hamiltonian in the relevant energy range $c^2 < E < V_0 - c^2$. There are two energy degenerate eigenstates $\Psi_e(E; x)$ and $\Psi_p(E; x)$, such that $H_{ATP} \Psi_{e,p}(E; x) = E \Psi_{e,p}(E; x)$ where

$$\begin{aligned} \Psi_e(E; x) = & \left[\exp(i k x) + A_{e,u} \exp(-i k x) \right] L_u + B_{e,u} \exp(-\kappa x) R_u \\ & + C_{e,d} \exp(\kappa_d x) L_d + C_{e,d} \exp(-i k_d x) R_d \end{aligned} \quad (3.2a)$$

$$\begin{aligned} \Psi_p(E; x) = & C_{p,u} \exp(-i k x) L_u + C_{p,u} \exp(-\kappa x) R_u \\ & + B_{p,d} \exp(\kappa_d x) L_d + \left[\exp(i k_d x) + A_{p,d} \exp(-i k_d x) \right] R_d \end{aligned} \quad (3.2b)$$

Here we distinguish between the two spatial domains (left and right) and the spinor components (up and down) with the compact notations $L_u \equiv \theta(-x) (1,0)$, $R_u \equiv \theta(x) (1,0)$, $L_d \equiv \theta(-x) (0,1)$ and $R_d \equiv \theta(x) (0,1)$. The four positive momenta are defined as $k \equiv [2(E-c^2)]^{1/2}$, $\kappa \equiv [2(V_0-E+c^2)]^{1/2}$, $\kappa_d \equiv [2(E+c^2)]^{1/2}$ and $k_d \equiv [2(V_0-E-c^2)]^{1/2}$. It is important that due to the coupling λ , both spinor components have to be non-zero. While the upper spinor component of $\Psi_e(E; x)$ describes the wave function for an incoming electron with amplitude 1 that scatters off of the potential step and tunnels to $x > 0$, the lower component describes a particle coming in from the right side [note that $\exp(i k_d x)$ describes a left moving particle] and tunnels to $x < 0$.

By assuming the usual continuity $\Psi(E; x-\epsilon) = \Psi(E; x+\epsilon)$ and also the discontinuity of the derivative required for this Hamiltonian, $\partial_x \Psi(E; x+\epsilon) = \partial_x \Psi(E; x-\epsilon) + 2i\lambda \sigma_2 \Psi(E; x=0)$, we can construct the six coefficients as

$$A_{e,u} = [(k_d - i \kappa_d)(k - i \kappa) - 4\lambda^2] D \quad (3.3a)$$

$$B_{e,u} = 2 k (k_d - i \kappa_d) D \quad (3.3b)$$

$$C_{e,d} = -4 i \lambda k D \quad (3.3c)$$

$$A_{p,d} = [(k_d + i \kappa_d)(k + i \kappa) - 4\lambda^2] D \quad (3.3d)$$

$$B_{p,d} = 2 k_d (k + i \kappa) D \quad (3.3e)$$

$$C_{p,u} = -4 i \lambda k_d D \quad (3.3f)$$

with the common denominator $D \equiv 1/[(k_d - i \kappa_d)(k + i \kappa) + 4\lambda^2]$. These amplitudes can be directly related to each other by exchanging the spinor labels u and d and complex conjugation. This symmetry leads to an interesting relationship between both states.

While due to the degeneracy any superposition of $\Psi_e(E;x)$ and $\Psi_p(E;x)$ is an energy eigenstate, the two specific states in Eqs. (3.2) were chosen with regard to their coupling-free ($\lambda=0$) limit, that allows us to uniquely distinguish between electronic and positronic states. This unique identification of particle states is not trivial for the degenerate states from the Dirac equation, where all spinor components are mixed even for $V_0=0$. Here the corresponding eigenstates $\Psi_e(E;x,\lambda=0) \sim (1,0)$ and $\Psi_p(E;x,\lambda=0) \sim (0,1)$ have purely electronic and positronic forms, corresponding to vanishing spinor components $C_{e,d}=0$ and $C_{p,u}=0$.

$$\Psi_e(E;x,\lambda=0) = [\exp(i k x) + A'_{e,u} \exp(-i k x)] L_u + B'_{e,u} \exp(-\kappa x) R_u \quad (3.4a)$$

$$\Psi_p(E;x,\lambda=0) = B'_{p,d} \exp(\kappa_d x) L_d + [\exp(i k_d x) + A'_{p,d} \exp(-i k_d x)] R_d \quad (3.4b)$$

where the primed coefficients are identical as in Eqs. (3.3), except that $\lambda=0$.

Here they simplify significantly to $A'_{e,u} = (k - i \kappa)/(k + i \kappa)$, $B'_{e,u} = 2k/(k + i \kappa)$, $A'_{p,d} = (k_d + i \kappa_d)/(k_d - i \kappa_d)$ and $B'_{p,d} = 2k_d/(k_d - i \kappa_d)$.

For conceptual simplicity we have assumed that the part of the wave functions that represent the incoming particles have unit amplitude. As a result the states are not normalized correctly. In Appendix A we show how we can approximate the overall normalization factors as $N = [2\pi |k_u]|^{-1/2}$, such that these states can be normalized on an energy scale such that we have $\langle \Psi(E_1) | \Psi(E_2) \rangle = \delta(E_1 - E_2)$.

As it plays a key role for the calculation of the pair creation rate (as shown in Sec. 3.2), we determine next the transmission coefficient. This will also permit us a first comparison of the predictions of the ATP Hamiltonian with the Dirac Hamiltonian. Using the functional

dependence of the coefficients in Eq. (3.3a), we can derive it by the ratio of the incoming and transmitted current as $T(E) = j_{\text{trans}}/j_{\text{inc}}$, we obtain $T_{\text{ATP}}(E) = k_d |C_{e,d}|^2 / k = k |C_{p,u}|^2 / k_d = 16 \lambda^2 k k_d |D|^2$. The non-monotonic dependence of $T_{\text{ATP}}(E)$ on the coupling force strength $T_{\text{ATP}}(E) \sim \lambda^2 / |z + 4\lambda^2|^2$ indicates that there are also two competing mechanisms associated with the force term $\lambda \delta(x) \sigma_1$. For small λ , it increases the transmission (as $C_{e,d}$ increases with λ) but for larger λ the same force term leads also to an increased reflection (as $A_{e,u}$ increases with λ and therefore $C_{e,d}$ decreases), effectively decreasing the transmission. As the result, there is an optimum coupling strength for each energy, $\lambda = |z|^{1/2}/2 = |[(k_d - i \kappa_d)(k + i \kappa)]^{1/2}/2$ that maximizes the transmission. For $E=1.5c^2$ it amounts to $0.816 V_0/(2c)$, which coincidentally happens to be close to the amplitude $V_0/(2c)$ from Eq. (2.2). For simplicity, we choose $V_0/(2c)$ from now on.

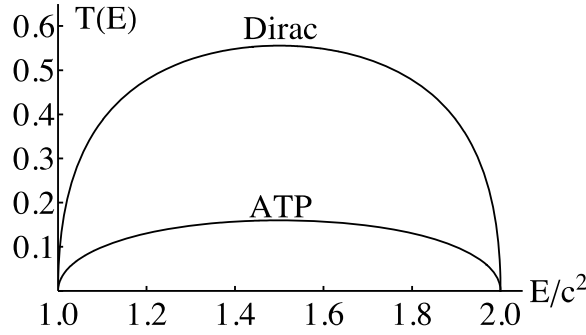


Figure 1. Comparison of the quantum mechanical transmission coefficients $T(E)$ obtained from the original Dirac and ATP Hamiltonian for a supercritical potential step of height $V_0 = 3c^2$. We used a coupling strength $\lambda = V_0/(2c)$ for the ATP Hamiltonian.

In Figure 1 we have compared this coefficient with the well-known one [22] obtained from the corresponding Dirac equation approach. It is given by $T_D(E) = 2 c^2 p q / [E(V_0 - E) + c^2 p q + c^4]$, where the relativistic momenta are $p \equiv (E^2 - c^4)^{1/2}/c$ and $q \equiv [(V_0 - E)^2 - c^4]^{1/2}/c$. In the non-relativistic limit ($c \rightarrow \infty$) we have $p \rightarrow k$ and $q \rightarrow k_d$. We see that all essential features such as the energy range, $c^2 < E < V_0 - c^2$, and the location of a single maximum at $E = V_0 + c^2/2$ can be qualitatively reproduced by the Hamiltonian H_{ATP} . This gives us some confidence that basic features of the pair creation process can be described by this (more transparent) model.

There are two mechanisms that could be responsible for the observed difference between $T_D(E)$ and $T_{\text{ATP}}(E)$ in Fig. 1. A Hamiltonian with the kinetic operator $(c^2 + p^2/2) \sigma_3$ permits the

occurrence of velocities that can exceed c , whereas any velocity in the Hamiltonian with a (relativistic) kinetic operator of the form $(c^4 + c^2 p^2)^{1/2} \sigma_3$ has to obey the speed limit $v < c$. So if hypothetically the external force would excite the same momentum states in both systems, in the non-relativistic description this would correspond to higher velocities. As faster particles can leave the pair creation zone more effectively this mechanism by itself would increase the pair creation rate and therefore would predict $T_D(E) < T_{ATP}(E)$, which, however, is not observed in the simulation. The original potential $V(x)$ was chosen piecewise constant but the unavoidable delta functions in x [associated in the higher derivatives of $V(x)$] contained in the two potentials F_{diag} and F_{off} in Eq. (2.2) were omitted in H_{ATP} . We therefore conjecture that the larger Dirac transmission coefficient $T_D(E)$ is due to these omitted terms.

3.2 The ATP pair creation rate for the potential step

Finally, we use all of this information to show how the pair creation rate is directly related to the transmission coefficient $T(E)$. As shown above, the number of created electrons with energy E as a function of time can be defined by projecting the time-evolved ATP-Dirac sea states $|d;p\rangle$ on the states of the upper energy continuum, $N(E;t) \equiv \int dE' |\langle u;E | \exp(-i H_{ATP} t) |d;E'\rangle|^2$. We can replace the force-free state $\langle u;E |$ with twice the true energy eigenstate $\langle \Psi(E) |$ of the ATP Hamiltonian. The factor of 2 is due to the fact that $\langle \Psi(E) | u;E'\rangle$ is close to $\frac{1}{2} \delta(0)$. The action of H_{ATP} on $\langle \Psi(E) |$ reproduces the energy $\exp(-i E t)$, leading to $N(E;t) = \int dE' 4 |\langle \Psi(E) | d;E'\rangle|^2$ that seems to have become independent of time. However, the inner product expressed as a spatial integral yields an important delta function in the energy

$$\begin{aligned}
\langle \Psi(E) | d;E'\rangle &= N N_f \int_{-\infty}^0 dx [C_{e,d}^* \exp(\kappa_d x + i k_n x)] + \int_0^{\infty} C_{e,d}^* \exp(i k_d x + i k_n x)] \\
&= N N_f \{ C_{e,d}^* (\kappa_d + i k_n)^{-1} + C_{e,d}^* [\pi \delta(k_d + k_n) + i/(k_d + k_n)] \} \\
&\approx N N_f C_{e,d}^* \pi \delta(k_d + k_n) \\
&= N N_f C_{e,d}^* \pi |k_d| \delta(E - E_n)
\end{aligned} \tag{3.5}$$

where we have dropped the principal parts. If we square the absolute value of Eq. (3.5) and use $\delta(E - E_n)^2 = \delta(E - E_n) \delta(E = 0)$ and $\delta(E = 0) = t (2\pi)^{-1}$, we obtain

$$N(E,t) = 4 |N_f C_{e,d} \pi k_d|^2 (2\pi)^{-1} t \equiv \Gamma(E) t \quad (3.6)$$

If we then insert the normalization constant (derived in Appendix A) the resulting expression for the pair creation yield simplifies significantly and we obtain the final result

$$\Gamma(E) = (2\pi)^{-1} T(E) \quad (3.7)$$

where $T(E)$ is the quantum mechanical transmission coefficient derived above. This relationship was first conjectured by Hund [13].

This result is rather interesting and confirms the usual Hund rule, which for the case of the Dirac equation relates the pair creation rate directly to the corresponding transmission coefficient, is also valid for the ATP system. In order to test the validity of both proposed analytical expressions (and the approximations in its derivation) we have computed the number of created electrons $N(E;t)$ ab initio from a time-dependent simulation of the dynamics. For the computational details of these ab-initio simulations, see [9,10,20,22-26]. In order to describe numerically an abrupt potential step, we have actually used a smooth $\tanh(x/w)$ -like step [27] with the very narrow turn on width of $w=0.01/c$.

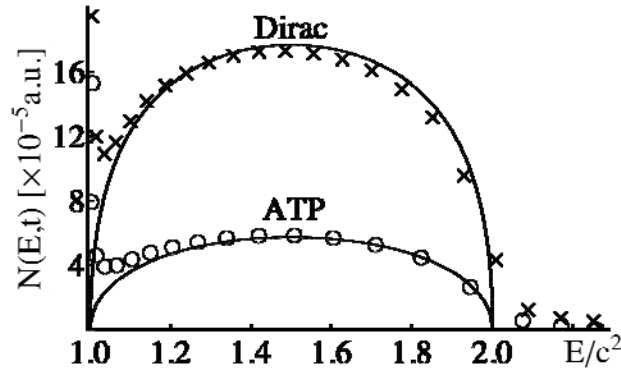


Figure 2. The energy dependence of the number of created electrons $N(E,t)$ per energy at time t obtained from ab-initio simulations of the pair-creation process based on the Dirac and the ATP Hamiltonian. The continuous data are the predictions $N(E,t) = \Gamma(E) t$ based on the asymptotic long-time rate, which can be obtained analytically. [$t=2 \times 10^{-3}$ a.u., same parameters as in Fig. 1]

The true energy distribution of the emitted particles $N(E,t)$ at time t is the accumulated result

of several pair creation mechanisms. At early times, $N(E,t)$ covers a wide energy range associated with temporally induced transitions associated with the abrupt turn on of the external force field. This leads to many low energy electrons as well as electrons with energies that exceed $2c^2$, but the distribution decreases monotonically with E . The asymptotic long-time pair creation regime is characterized by the circularly shaped distribution, whose maximum occurs at energy $E_{\max}=V_0/2$. As we have derived above, this distribution can be derived analytically from the transmission coefficient, $N(E,t) = (2\pi)^{-1} T(E) t$. The data in Figure 2 show nicely how the true yields evolve in their asymptotic form for the Dirac as well as ATP Hamiltonian.

If we integrate the long-time energy spectrum over all energies, we can also obtain the total pair creation rate, $N(t) = \int dE \Gamma(E) t \equiv \Gamma t$. While for the ATP dynamics the numerical data for $N(t)$ predicts a slope of about $dN(t)/dt = 388$ a.u., the integral $(2\pi)^{-1} \int dE T(E)$ amounts to 381 a.u., leading to a relative difference of less than 2%, which is fully consistent with the expected numerical accuracy of the computational simulations.

We should finish this section by pointing out an important difference between the Dirac and the ATP vacuum rate with respect to their perturbative nature. For an infinitely extended system, the functional dependence of the Schwinger rate on the electric field is non-perturbative as it cannot be Taylor expanded for small field amplitudes. Even for a finite system, such as the step potential, the corresponding Dirac rate is also non-perturbative. In this case the nonperturbative character is due to the fact that the rate is discontinuous in V_0 as it has to exceed a certain threshold value of $2c^2$ to become supercritical. In contrast, as we have derived above, the rate of the ATP Hamiltonian $\Gamma_{\text{ATP}}(E) \sim \lambda^2/|z+4\lambda^2|^2$ is a differentiable function of the coupling force strength λ and therefore fully perturbative.

4. Pair creation triggered by a spatially extended electric field

We will argue below that for more general and spatially extended external fields, the ATP Hamiltonian can offer some conceptual advantages over the usual approach based on the Dirac equation. To have a concrete example, we examine the simplest case of an extended region $0 < z < w$ where the external electric field is constant. The well-known Schwinger rate for an infinitely extended electric field [11] predicts that the pair creation yield depends on the electric field amplitude, which might suggest, that in our case the entire spatial region $0 < x < w$ should be able to create particles. However, the data obtained from the ATP Hamiltonian suggests that this

is not necessarily true. In Section 4.1 we examine first the time-dependence of the energy distribution of the emitted particles and in 4.2 we connect it to their spatial probability density.

4.1 Time-dependence of energy distribution of the emitted electrons

In this section we will examine if the predictions based on the analytical expressions obtained for the step potential are also useful for understanding the pair creation for spatially extended electric fields. The corresponding ATP Hamiltonian for the potential that grows linearly in space for $0 < x < w$ and then remains constant $V(x) = V_0$ for $w < x$ is given by

$$H_{\text{ATP}} = (c^2 + p^2/2) \sigma_3 + V_0 [x/w \theta(x)\theta(w-x) + \theta(x-w)] \sigma_0 + V_0/(2wc) \theta(x)\theta(w-x) \sigma_1 \quad (4.1)$$

It describes a spatial region $0 < x < w$, where –at least in principle– the pair creation can occur at all times. A comparison of the exact data obtained from a direct ab-initio simulation will permit us to examine if the specific functional dependence of the pair creation rate and the spatial probability density on the transmission coefficient can be generalized to spatially extended force fields. To do so we have to compute first the corresponding transmission coefficient $T(E)$ for the linear ramp potential for the ATP Hamiltonian. This can be accomplished numerically by an iteration method that we detail in Appendix B.

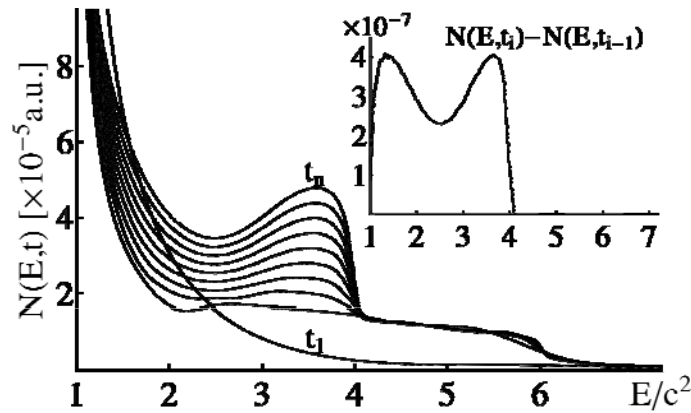


Figure 3. Temporal growth of the energy spectra of the created electrons $N(E,t)$ for a spatially extended force field obtained from ab-initio simulations of the pair-creation process based on the ATP Hamiltonian. The chosen moments in time are $t_n = n \Delta t + 5 \times 10^{-5}$ a.u., where $\Delta t = 3 \times 10^{-4}$ a.u. and $n = 1, 2, \dots, 10$. The inset shows the differences of two consecutive distributions for $i = 9$ and 10 . [$V_0 = 5c^2$, $w = 5/c$].

In Figure 3 we display the energy spectra of the emitted electrons $N(E,t)$ at various moments in time for the potential with $V_0=5c^2$. Similarly to the case of the step potential, at early times the distribution falls off exponentially with energies covering a wide range. The corresponding electrons were partly created due to the unavoidable time-dependence of the electric field during its rapid turn on. At longer times the permanent and supercriticality-based creation mechanism dominates, leading also to a linear growth of the total number of particles, $N(t) = \int dE N(E,t) = \Gamma t + \alpha$. Here we measured the rate $\Gamma=59.52$ a.u., which agrees very well with the rate as predicted from the transmission coefficient, $(2\pi)^{-1} \int dE T(E) = 59.79$ a.u.. This confirms once again the relationship of Eq. (3.7) between $T(E)$ and the rate $\Gamma(E)$ for the ATP Hamiltonian for finite electric fields.

The electrons created by the steady-state mechanism take only energies in the smaller range $c^2 < E < 4c^2$. To illustrate this, we have subtracted out the contributions from earlier times and graphed in the inset the difference $N(E,t_i) - N(E,t_{i-1})$ for two times corresponding to $i=9$ and $i=10$. The two differences are identical, as expected for the pair creation process in its steady state. For very small time-increments, these differences (when divided by $t_{i+1} - t_i$) should match the energy dependence of the pair creation rate $\Gamma(E)$.

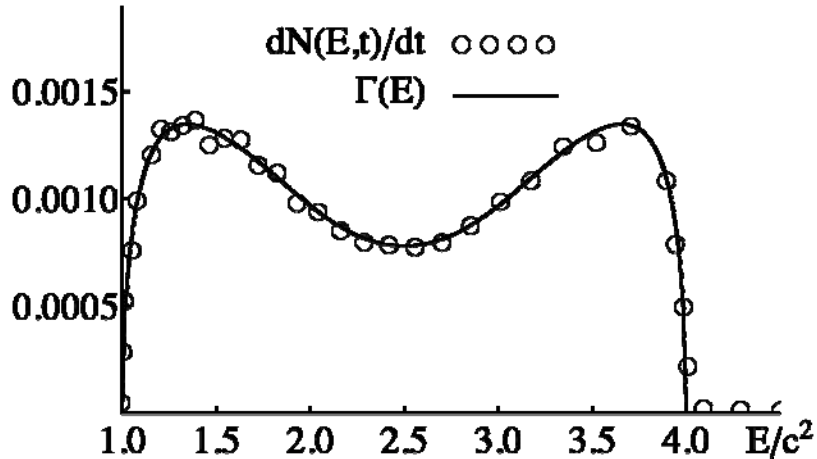


Figure 4. The energy dependence of the pair creation rate $dN(E,t)/dt$ per energy at time t for a spatially extended force field obtained from ab-initio simulations of the pair-creation process based on the ATP Hamiltonian. The continuous data are the predictions for $\Gamma(E)$ based on the transmission coefficient for this potential.

To make this comparison more quantitative, we compare in Figure 4 the true pair creation rate obtained from the long time limit of the ab-initio simulation with the corresponding expression $\Gamma(E)$ for the ATP equation. We see that the agreement between the exact data and the long-time approximation based on the transmission coefficient is excellent also for a spatially extended force field. In contrast to the rate for the potential step (Fig. 2) that was centered around a single maximum at energy $V_0/2$, the rate for the extended electric field has now two maxima. The magnitude of the rate $\Gamma(E)$ is the result of the density of the states that is decreasing with the energy difference from $E=c^2$ (for the electronic states) and from $E=V_0-c^2$ (for the positronic states). It also depends on the scalar product between the electronic and positronic states and therefore their penetration (tunneling) depth into the region $0 < x < w$.

In the next section we will argue that using the dressed (but uncoupled energy eigenstates) suggests that this narrow energy production range ($c^2 < E < V_0 - c^2$) correlates directly with a restricted spatial range inside the force region where particles can be created.

4.2 Spatial dependence of the created electrons

In several prior works [9,10,20,28,29], the force-free energy eigenstates $|u;p\rangle$ and $|d;p\rangle$ were used to compute the spatial probability distribution $\rho(x,t)$ of the created electrons as

$$\rho_{\text{free}}(x,t) \equiv \left| \int dE' \int dE \langle u;E | \exp(-i Ht) | d;E' \rangle (2\pi |k|)^{-1} \exp(ik x) \right|^2 \quad (4.2)$$

However, we remark that there were also works that do not rely on these states and examined different projections in order to identify particles. Gerry et. al. [30] have used dressed states but for a special case where the particles were created exclusively due to a time-dependent electric field. A similar scenario was studied in 2010 by Mocken et al. [31]. During the same year, Hebenstreit et al [32] provided space-resolved information using a Wigner function formalism. In 2014 Dabrowski and Dunne [33] outlined a new scheme to overcome the ambiguity of defining vacua at finite times by using a superadiabatic particle number according to Berry's universal smoothing of the Stokes phenomenon.

The spatial distribution inside the pair creation zone cannot be accurately described by this expression (4.2), as the force-free states and $|d;E\rangle$ are not so easy to be interpreted in regions where the force does not vanish. We therefore propose to examine an alternative definition for

$\rho(x,t)$, where these states are replaced by the electronic energy eigenstates of the ATP Hamiltonian for $\lambda=0$, denoted by $|\Psi(E;\lambda=0)\rangle$. Furthermore, we replace $\langle x|u;E\rangle = (2\pi|k|)^{-1} \exp(ikx)$ by the dressed wave function $\Psi_p(E;x,\lambda=0)$. Similarly as in Eq. (3.1), we have introduced the coupling parameter λ to separate between the effects due to the dressing [associated with the diagonal potential in Eq. (4.1)] and the actual creation of particles with strength λ given by the last term in Eq. (4.1). This state was obtained numerically by diagonalization of the ATP Hamiltonian for $\lambda=0$ on a spatial grid [34]. Their analytical structure for the potential step, [given by Eq. (3.4a) above] showed that electrons decaying exponentially in the energetically forbidden domain where $E < V(x)$, which we also expect to be true for the extended force fields. However for our extended field there is the additional interesting region $0 < x < w$, where the potential grows linearly. Based on these states we can define

$$\rho_{\text{ATP}}(x,t) \equiv \int dE' \left| \int dE \langle \Psi_e(E;\lambda=0) | \exp(-i Ht) | d;E' \rangle \Psi_e(E;x,\lambda=0) \right|^2 \quad (4.3)$$

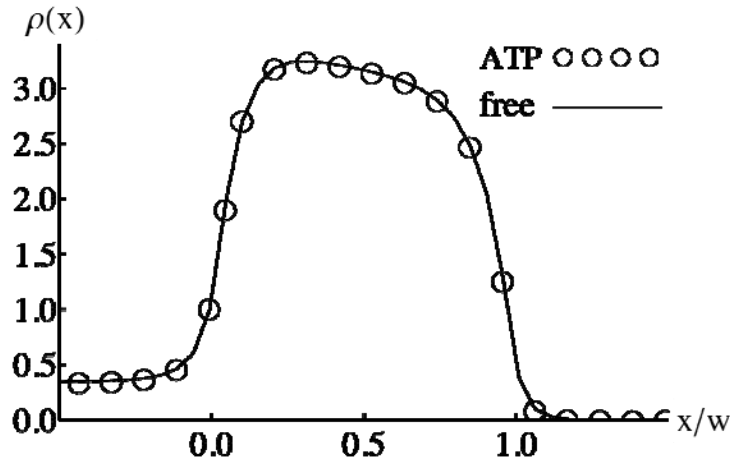


Figure 5. The spatial probability density of the electrons in the steady state $\rho_{\text{free}}(x)$ and $\rho_{\text{ATP}}(x)$ based on the force-free and dressed states of Eqs. (4.2) and (4.3). [Parameters as in Fig. 4]

We should note that while Eq. (4.2) assumed that the initially occupied Dirac sea consists of force-free states [negative energy eigenstates of $(c^2+p^2/2) \sigma_3$], the modified definition Eq. (4.3) assumes that the initial quantum field theoretical state corresponds to the vacuum associated with the dressed (but uncoupled) Hamiltonian $(c^2+p^2/2) \sigma_3 + V_0 [x/w \theta(x)\theta(w-x) + \theta(x-w)] \sigma_0$.

In Figure 5 we compare the steady state distributions $\rho_{\text{free}}(x)$ and $\rho_{\text{ATP}}(x)$ for the same

dynamics as discussed in Section 4.1. Quite remarkably, the two probabilities are graphically indistinguishable, which is unexpected at first as the underlying states $|d;E\rangle$ and $|\Psi_p(E;\lambda=0)\rangle$ have entirely different structures for $0 < x$, especially inside the important force region $0 < x < w$. In fact even at earlier times we found that the time dependence of the total particle yield, given by the spatial integral as $N(t) = \int dx \rho(x,t)$, was identical. This agreement is not so unexpected, as the two Hilbert spaces spanned by *all* initially occupied states $|d;E\rangle$ and $|\Psi_p(E;\lambda=0)\rangle$ are identical. In other words, both represent the same quantum field theoretical vacuum state. It should be obvious that if we had used the exact vacuum state, corresponding to an ATP Dirac sea spanned by all occupied states $|\Psi_p(E;\lambda)\rangle$, no particle pairs would be observed.

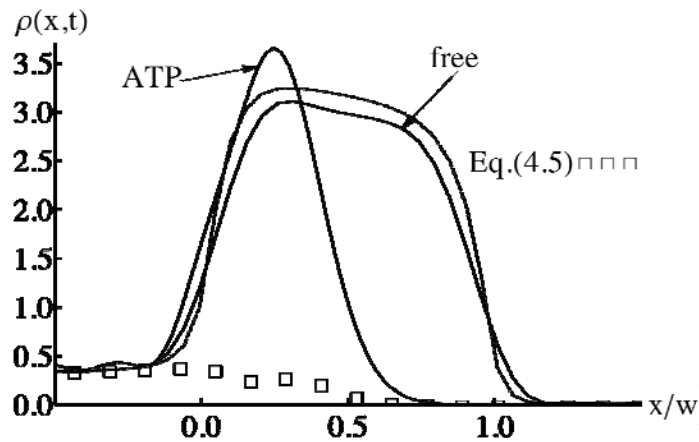


Figure 6. The spatial probability density of the electrons in the steady state $\rho_{\text{free}}(x)$ and $\rho_{\text{ATP}}(x)$ created from the force-free and dressed vacuum state. However, in contrast to Figure 5, the energy range of the permitted states has been reduced to $c^2 < E < 4c^2$. For comparison, the dashed line shows $\rho_{\text{free}}(x)$ (see Fig. 5) that was computed without any energy reduction. The squares are the predictions based on the quasi-analytical approximation from Eq. (4.5) [Parameters as in Fig. 4]

In order to test if it is possible to identify spatial domains where the electrons are created inside the force region, we have truncated the energy integration interval in Eq. (4.2) and (4.3) to $c^2 < E < 4c^2$. The resulting steady state distributions $\rho_{\text{free}}(x)$ and $\rho_{\text{ATP}}(x)$ are shown in Figure 6. While the two probabilities -when computed over the entire energy range- were identical (see Fig. 5), there are now a significant differences between the two approaches used to compute $\rho(x)$. The force-free states based distribution $\rho_{\text{free}}(x)$ is overall lowered (compared to the untruncated dashed line of Fig. 5). If $\rho_{\text{free}}(x)$ would describe true physical particles inside the field, this

would suggest that even in the steady state electrons can be created in the entire spatial range $0 < x < w$. However, this is not true at all as the modified spatial density $\rho_{\text{ATP}}(x)$ based on the dressed states shows. Here the energy reduction to $c^2 < E < 4c^2$ clearly shows that the occupation of the spatial region $0.6w < x < w$ observed in $\rho_{\text{free}}(x)$ and $\rho_{\text{ATP}}(x)$ is entirely due to earlier times long before the steady state has developed. In fact, by removing the contribution of energy states with $E > 4c^2$ from $\rho_{\text{ATP}}(x)$, removes automatically also all electrons from $0.6w < x < w$. This observation is also fully consistent with the data $N(E,t)$ shown in Figs. 3 and 4 that proved that energies $E > 4c^2$ cannot be created at longer times.

This means, that there is a spatial domain in the long-time (steady-state) limit where no particles can be created, even though the external force is non-zero in the entire region $0 < z < w$. The existence of the shorter pair creation region $[0 < x < w(1 - 2c^2 V_0^{-1})]$ suggests that the amount of the local force is not solely determining how many electrons are created there. A nontrivial question, however, remains why these earlier created high-energy “electrons” did not accelerate out of the pair creation zone. Here it is important to understand that a non-zero density $\rho_{\text{free}}(x)$ should not be directly associated with the existence of physical particles inside the force zone. Several prior works [30,35] have discussed this conceptual issue in more detail.

The advantage of the ATP-based basis states over the free states also permits us to examine an approximate but quasi-analytical approach to the steady state $\rho(x)$. It turns out that we can use this expression to approximate the long-time asymptotic distribution. If we replace the states $|\Psi_e(E; \lambda=0)\rangle$ with the corresponding true energy eigenstates $|\Psi_e(E; \lambda)\rangle$, the action of the time evolution operator can be applied

$$\rho(x,t) \equiv \int dE' \left| \int dE \langle \Psi_e(E; \lambda=0) | \exp(-i H t) | \Psi_p(E; \lambda=0) \rangle \Psi_e(E; \lambda=0) \right|^2 \quad (4.4)$$

In the limit of long times we can approximate this by $\rho(x,t) \approx \int dE' \left| \int dE \exp(-i E t) \langle \Psi_e(E; \lambda) | \Psi_p(E; \lambda=0) \rangle \Psi_e(E; \lambda=0) \right|^2$. We can use similar approximations as we used for the step potential, and obtain the proportionality

$$\rho(x) \sim \int dE \Gamma(E) |\Psi_e(E; x, \lambda=0)|^2 \quad (4.5)$$

We obtain the interesting and rather intuitive result that the spatial steady state density is just the integral over the density of each electronic energy eigenstate with a weight factor that is proportional to the energy-dependent pair creation rate $\Gamma(E)$.

In order to test this rather serious sequence of approximations, we have included the predictions of Eq. (4.5) in Figure 5 by the open squares. It predicts correctly the constant density of outgoing particles for $x < 0$. In contrast to $\rho_{\text{free}}(x)$ and $\rho_{\text{ATP}}(x)$, which increase first inside the force-region, Eq. (4.5) suggests that inside the potential the density decays monotonically until it vanishes for $0.6w < x$. We believe that this unphysical increase is related to the same conceptual difficulty as the permanent occupation of the spatial region $w(1-2c^2V_0^{-1}) < x < w$.

5. Summary and brief outlook

We have introduced an approximate but illustrative model Hamiltonian that can predict the creation of electron-positron pairs. Its main advantage compared to the more fundamental and accurate description in terms of the traditional Dirac Hamiltonian is the separation of the external force field into contributions that solely provide the spatial evolution of the particles and a second (off-diagonal) part that is solely responsible for their creation.

We have seen that the availability of the dressed particle states for ($\lambda=0$) can provide a much better basis to compute spatial densities than the usual force-free states. For example, the spatial densities inside the pair creation zone characterized by a constant force revealed that there are spatial regions where particles cannot be created at all. To improve the transparency of these spatial densities even more, one could project the electron field operator on the full energy eigenstates of the system. However, in this case the densities are no longer time dependent.

There are several fascinating questions that can be addressed in future works. It is very interesting to examine the relative importance of the diagonal and off-diagonal potential for the pair creation yield. If we repeat the simulation of Sec. 4 but remove the diagonal-potential completely from the dynamics, the time-dependence of the number of created particles is oscillates around zero. As the particles do not interact directly with each other and they are born basically at rest, they have no means of leaving the interaction zone. As a result, we have repeated sequences of pair creation followed by complete annihilation and as a net result no permanent pair creation. In this sense the diagonal part of the potential is crucially important for pair creation by facilitating the particles' permanent separation.

The ATP Hamiltonian was derived only in the lowest nonvanishing order of the momentum. It might be very interesting to calculate higher order term in the potential and examine if they have a similarly straightforward interpretation with regard to their role for the pair creation process. It is presently not clear if these additional terms would contain higher spatial derivatives of the original potential or if they would contain also the momentum operator. As similar higher-order analysis might also be interesting in three-spatial dimensions, where the vector potential could describe effects due to an external magnetic field.

Acknowledgements

QZL would like to thank ILP for the nice hospitality during his visit to Illinois State. This work has been supported by the NSF, the NSFC (#11529402) and the National Basic Research Program of China (2013CBA01501).

Appendix A The normalization of the scattering states of the ATP Hamiltonian

In this appendix we compute the normalization coefficients such that the energy eigenstates of the ATP Hamiltonian are energy normalized, e.g. $\langle \Psi(E_1) | \Psi(E_2) \rangle = \delta(E_1 - E_2)$. In the trivial case of the force-free states $|d; E\rangle = N_f \exp(ikx)$ (0,1), this amounts to $N_f = (2\pi |k|)^{-1/2}$ such that $\langle d; E_1 | d; E_2 \rangle = \delta(E_1 - E_2)$. Using the notation defined in the main text, we found the (non-normalized) states of the full ATP Hamiltonian for the zero-range potential

$$\begin{aligned} \langle x | \Psi(E) \rangle = & \exp(ik_u x) L_u(x) + A_{e,u} \exp(-ik_u x) L_u(x) + B_{e,u} \exp(-\kappa_u x) R_u(x) \\ & + C_{e,d} \exp(\kappa_d x) L_d(x) + C_{e,d} \exp(-ik_d x) R_d(x) \end{aligned} \quad (A1)$$

If we express the inner product $\langle \Psi(E_1) | \Psi(E_2) \rangle$ as an integral over the position space we obtain

$$\begin{aligned} \langle \Psi(E_1) | \Psi(E_2) \rangle = & \int_{-\infty}^0 dx \left\{ [\exp(-ik_{u1}x) + A_{e,u1}^* \exp(ik_{u1}x)] [\exp(ik_{u2}x) + A_{e,u2} \exp(-ik_{u2}x)] + \right. \\ & \left. + C_{e,d1}^* C_{e,d2} \exp(\kappa_{d1}x + \kappa_{d2}x) \right\} + \\ & + \int_0^{\infty} dx \left\{ B_{e,u1}^* B_{e,u2} \exp(-\kappa_{u1}x - \kappa_{u2}x) + C_{e,d1}^* C_{e,d2} \exp(ik_{d1}x - ik_{d2}x) \right\} \end{aligned} \quad (A2)$$

multiplying the factors we obtain the following seven integrals over the half-space. Using the general equality $\int_0^{\infty} dx \exp(ikx) = \pi \delta(k) + i/k$, these integrals can be evaluated to the sum of the delta function and the principal part,

$$\begin{aligned} \langle \Psi(E_1) | \Psi(E_2) \rangle = & \int_{-\infty}^0 dx [\exp(ik_{u2}x - ik_{u1}x) + A_{e,u1}^* A_{e,u2} \exp(ik_{u1}x - ik_{u2}x)] + \\ & + \int_{-\infty}^0 dx [A_{e,u2} \exp(-ik_{u1}x - ik_{u2}x) + A_{e,u2}^* \exp(ik_{u1}x + ik_{u2}x)] + \\ & + \int_{-\infty}^0 dx C_{e,d1}^* C_{e,d2} \exp(\kappa_{d1}x + \kappa_{d2}x) + \\ & + \int_0^{\infty} dx B_{e,u1}^* B_{e,u2} \exp(-\kappa_{u1}x - \kappa_{u2}x) + \\ & + \int_0^{\infty} dx C_{e,d1}^* C_{e,d2} \exp(ik_{d1}x - ik_{d2}x) \\ = & [\pi \delta(k_{u2} - k_{u1}) - i/(k_{u2} - k_{u1})] + A_{e,u1}^* A_{e,u2} [\pi \delta(k_{u1} - k_{u2}) - i/(k_{u1} - k_{u2})] + \end{aligned}$$

$$\begin{aligned}
& + A_{e,u2} [\pi \delta(k_{u1}+k_{u2}) - i/(-k_{u1}-k_{u1})] + A_{e,u2}^* [\pi \delta(k_{u1}+k_{u2})-i/(k_{u1}+k_{u1})] + \\
& + C_{e,d1}^* C_{e,d2} (\kappa_{d1} + \kappa_{d2})^{-1} + \\
& + B_{e,u1}^* B_{e,u2} (\kappa_{u1} + \kappa_{u2})^{-1} + \\
& + C_{e,d1}^* C_{e,d2} [\pi \delta(k_{d1}-k_{d2}) + i/(k_{d1}-k_{d2})] \tag{A3}
\end{aligned}$$

We need to introduce the normalization factor such that $\langle \Psi(E_1) | \Psi(E_2) \rangle = \delta(E_1 - E_2)$. We can therefore drop the non-resonant delta functions, the principal parts and the constant terms

$$\begin{aligned}
\langle \Psi(E_1) | \Psi(E_2) \rangle & = \pi \delta(k_{u2}-k_{u1}) + |A_{e,u1}|^2 \pi \delta(k_{u1}-k_{u2}) + |C_{e,d1}|^2 \pi \delta(k_{d1}-k_{d2}) \\
& = \pi \delta(k_{u2}-k_{u1}) + |A_{e,u1}|^2 \pi \delta(k_{u1}-k_{u2}) + |C_{e,d1}|^2 \pi |k_{d1}/k_{u1}| \delta(k_{u1}-k_{u2}) \\
& = \pi |k_u| \delta(E_2-E_1) + |A_{e,u1}|^2 \pi |k_u| \delta(E_2-E_1) + |C_{e,d1}|^2 \pi |k_d| \delta(E_2-E_1) \tag{A4}
\end{aligned}$$

We therefore find the normalization factor $N = [\pi |k_u| (1+|A_{e,u}|^2) + \pi |k_d| |C_{e,d}|^2]^{-1/2}$. If we use the definition of the coefficients for $A_{e,u}$ and $C_{e,d}$, this simplifies to $N = [2\pi |k_u|]^{-1/2}$.

Appendix B Numerical determination of the transmission coefficient

As the transmission coefficient plays such a central role in this work, we summarize here the numerical method that was used to compute it for a Hamiltonian. For simplicity of presentation, we illustrate the algorithm first for the Schrödinger equation with a brief test for a step potential and then provide the more complicated equations for the ATP Hamiltonian.

If we approximate the action of the spatial second derivative by a three-point finite difference formula, $d^2\Psi(x_{n-1})/dx_{n-1}^2 = [\Psi(x_{n-2}) - 2\Psi(x_{n-1}) + \Psi(x_n)]/\Delta x^2 + O(\Delta x^2)$, then the eigenvalue equation $[p^2/2 + V(x)]\Psi(x) = E \Psi(x)$ for a scattering state $\Psi(x)$ of chosen energy E can be expressed on a spatial lattice grid as

$$\begin{aligned}\Psi(x_n) &= 2 \Psi(x_{n-1}) - \Psi(x_{n-2}) + (2\Delta x^2) [-E \Psi(x_{n-1}) + V(x_{n-1}) \Psi(x_{n-1})] \\ &\equiv A_n \Psi(x_{n-1}) + B_n \Psi(x_{n-2})\end{aligned}\tag{B1}$$

where $A_n \equiv 2 + (2\Delta x^2) [V(x_{n-1}) - E]$ and $B_n \equiv -1$. In other words, it is an iterative scheme that permits us to derive consecutively the wave function on all grid points x_n , once one has chosen Ψ at the starting locations at x_1 and x_2 . The basic idea of the algorithm is to choose these two values $\Psi(x_1)$ and $\Psi(x_2)$ in such a way, that [for grid points x_1 and x_2 on the left side of the potential (where it is zero)] they match exactly the well-known structure for a scattering state, given by the sum of an incoming and a reflected state of energy $E = k^2/2$.

$$\Psi(x_1) = \exp(i k x_1) + r(k) \exp(-i k x_1)\tag{B2a}$$

$$\Psi(x_2) = \exp(i k x_2) + r(k) \exp(-i k x_2)\tag{B2b}$$

Here $r(k)$ denotes the momentum dependent reflection amplitude, whose determination is the ultimate goal of this algorithm. Here it is important to note that due to the linear structure of the Schrödinger equation with regard to Ψ , the functional relationship between the state and the reflection amplitude $r(k)$ maintains the general form $\Psi(x_n) = a_n + b_n r(k)$ for any spatial grid point. This means we can keep the value of $r(k)$ unspecified while the solution for $\Psi(x_n)$ is iteratively obtained by Eq. (B1). Instead of iterating $\Psi(x_n)$ directly from grid point x_n to x_{n+1} , we iterate the

two coefficients a_n and b_n with their two starting values $a_1 = \exp(ikx_1)$, $a_2 = \exp(ikx_2)$, $b_1 = \exp(-ikx_1)$ and $b_2 = \exp(-ikx_1)$. If we insert $\Psi(x_n) = a_n + b_n r(k)$ into Eq. (B1), we obtain $a_n + b_n r(k) = A_n [a_{n-1} + b_{n-1} r(k)] + B_n [a_{n-2} + b_{n-2} r(k)]$, or equivalently

$$a_n = A_n a_{n-1} + B_n a_{n-2} \quad (\text{B3a})$$

$$b_n = A_n b_{n-1} + B_n b_{n-2} \quad (\text{B3b})$$

This iterative scheme permits us to obtain the coefficients a_n and b_n (and therefore the eigenfunction) at all spatial grid points as a function of the (still unknown) reflection amplitude $r(k)$.

If we assume that the potential $V(x)$ takes a constant value at the final two grid points x_{N-1} and x_N , $V(x_{N-1})=V(x_N)=V_0$, then our scattering state that we are computing must take the precise functional form

$$\Psi(x_{N-1}) = t(k) \exp(i \kappa x_{N-1}) \quad (\text{B4a})$$

$$\Psi(x_N) = t(k) \exp(i \kappa x_N) \quad (\text{B4b})$$

where the lowered momentum over the barrier is defined as $\kappa \equiv [2(E-V_0)]^{1/2}$ and $t(k)$ is the momentum dependent transmission coefficient. After the iteration is completed, this leaves us with enough degrees of freedom to determine uniquely $r(k)$ and $t(k)$. We can therefore solve the two linear coupled equations

$$\Psi(x_{N-1}) = a_{N-1} + b_{N-1} r(k) = t(k) \exp(i \kappa x_{N-1}) \quad (\text{B5a})$$

$$\Psi(x_N) = a_N + b_N r(k) = t(k) \exp(i \kappa x_N) \quad (\text{B5b})$$

to obtain the desired transmission amplitude $t(t)$ from the numerical values for a_{N-1}, b_{N-1}, a_N and b_N as

$$t(k) = (a_{N-1} b_N - a_N b_{N-1}) / [b_N \exp(i \kappa x_{N-1}) - b_{N-1} \exp(i \kappa x_N)] \quad (\text{B6})$$

and therefore the transmission coefficient $T(E) = \kappa |t(k)|^2 / k$.

In order to briefly demonstrate the accuracy of this scheme, we have applied it to simple potential step, given by $V(x) = V_0 \theta(x)$ for which the analytical form of the transmission coefficient is known as $T(E) = 4 \kappa k / (k + \kappa)^2$. Using just four grid points $x_n = (n - 3/2)\Delta x$ for $n = 1, 2, 3, 4$ (corresponding to two iteration steps) we have tested the proposed interactive scheme. In Figure B1 we compare the numerical transmission coefficient with the exact form in the energy range $1 < E/V_0 < 1.5$ for three choices of the grid spacing Δx . We see that the method works superbly even for a discontinuous potential as long as Δx is chosen sufficiently small such that the three-point finite difference approximation is appropriate to describe the second derivative.

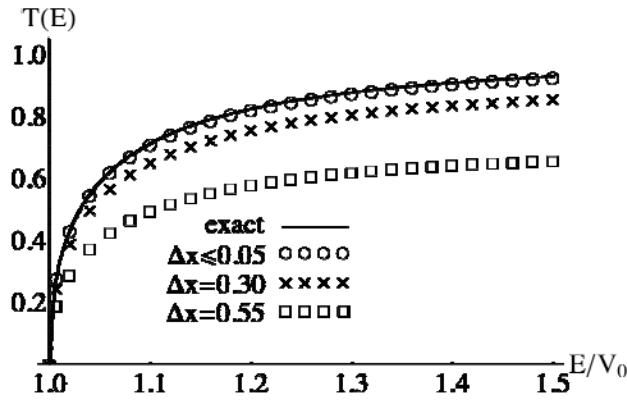


Figure B1. The transmission coefficient $T(E)$ for the test Hamiltonian $p^2/2 + V_0 \theta(x)$ for three spacings Δx used in the numerical algorithm. The continuous line is the exact analytical coefficient $T(E) = 4 \kappa k / (k + \kappa)^2$. [$V_0 = 2$ a.u.]

Due to the inherent generality of the algorithm, it can be used to compute the required transmission coefficient for the ATP Hamiltonian for any potential, given by the 2×2 matrix operator $H = (p^2/2 + c^2) \sigma_3 + V_{\text{diag}}(x) \sigma_0 + V_{\text{off}}(x) \sigma_1$. While the basic idea is the same, however, its concrete numerical implementation is more complicated as we have to iterate a two-component wave function in this case. The iterative scheme from Eq. (B1) corresponding to the eigenvalue equation generalizes to

$$\Psi_1(x_n) = A_{1,n} \Psi_1(x_{n-1}) + B_{1,n} \Psi_1(x_{n-2}) + C_{1,n} \Psi_2(x_{n-1}) \quad (\text{B7a})$$

$$\Psi_2(x_n) = A_{2,n} \Psi_2(x_{n-1}) + B_{2,n} \Psi_2(x_{n-2}) + C_{2,n} \Psi_1(x_{n-1}) \quad (\text{B7b})$$

with the six coefficients

$$A_{1,n} \equiv 2 + (2\Delta x^2) [V_{\text{diag}}(x_{n-1}) + c^2 - E] \quad (\text{B8a})$$

$$B_{1,n} \equiv -1 \quad (\text{B8b})$$

$$C_{1,n} \equiv (2\Delta x^2) V_{\text{off}}(x_{n-1}) \quad (\text{B8c})$$

$$A_{2,n} \equiv 2 - (2\Delta x^2) [V_{\text{diag}}(x_{n-1}) - c^2 - E] \quad (\text{B8d})$$

$$B_{2,n} \equiv -1 \quad (\text{B8e})$$

$$C_{2,n} \equiv - (2\Delta x^2) V_{\text{off}}(x_{n-1}) \quad (\text{B8f})$$

Among the two degenerate solutions, we are interested in finding the specific two-component eigenfunction for the problem that takes the general form for $x < 0$ where the potential is zero

$$\Psi_1(x) = \exp(i k x) + r_1(k) \exp(-i k x) \quad (\text{B9a})$$

$$\Psi_2(x) = r_2(k) \exp(\kappa_d x) \quad (\text{B9b})$$

where $k \equiv [2(E - c^2)]^{1/2}$ and $\kappa_d \equiv [2(E + c^2)]^{1/2}$ and $r_1(k)$ and $r_2(k)$ are unknown coefficients that depend nontrivially on the energy as well as the potential. We introduce again the corresponding six expansion coefficients

$$\Psi_1(x_n) = a_{1,n} + b_{1,n} r_1(k) + c_{1,n} r_2(k) \quad (\text{B10a})$$

$$\Psi_2(x_n) = a_{2,n} + b_{2,n} r_2(k) + c_{2,n} r_1(k) \quad (\text{B10b})$$

If we insert them into Eq. (B7) we find the following six iterative equations

$$a_{1,n} = A_{1,n} a_{1,n-1} + B_{1,n} a_{1,n-2} + C_{1,n} a_{2,n-1} \quad (\text{B11a})$$

$$b_{1,n} = A_{1,n} b_{1,n-1} + B_{1,n} b_{1,n-2} + C_{1,n} b_{2,n-1} \quad (\text{B11b})$$

$$c_{1,n} = A_{1,n} c_{1,n-1} + B_{1,n} c_{1,n-2} + C_{1,n} c_{2,n-1} \quad (\text{B11c})$$

$$a_{2,n} = A_{2,n} a_{2,n-1} + B_{2,n} a_{2,n-2} + C_{2,n} a_{1,n-1} \quad (\text{B11d})$$

$$b_{2,n} = A_{2,n} b_{2,n-1} + B_{2,n} b_{2,n-2} + C_{2,n} b_{1,n-1} \quad (\text{B11e})$$

$$c_{2,n} = A_{2,n} c_{2,n-1} + B_{2,n} c_{2,n-2} + C_{2,n} c_{1,n-1} \quad (\text{B11f})$$

If our solution was iterated correctly, it must take the following form at the two right most grid points (where the diagonal part of the potential is constant V_0 and the off-diagonals vanish).

$$\Psi_1(x_{N-1}) = a_{1,N-1} + b_{1,N-1} r_1(k) + c_{1,N-1} r_2(k) = t_1(k) \exp(-\kappa_u x_{N-1}) \quad (\text{B12a})$$

$$\Psi_2(x_{N-1}) = a_{2,N-1} + b_{2,N-1} r_1(k) + c_{2,N-1} r_2(k) = t_2(k) \exp(-i k_d x_{N-1}) \quad (\text{B12b})$$

$$\Psi_1(x_N) = a_{1,N} + b_{1,N} r_1(k) + c_{1,N} r_2(k) = t_1(k) \exp(-\kappa_u x_N) \quad (\text{B12c})$$

$$\Psi_2(x_N) = a_{2,N} + b_{2,N} r_1(k) + c_{2,N} r_2(k) = t_2(k) \exp(-i k_d x_N) \quad (\text{B12d})$$

Where the two momenta under the barrier are defined as $\kappa_u \equiv [2(V_{\text{diag}} - E + c^2)]^{1/2}$ and $k_d \equiv [2(V_{\text{diag}} - E - c^2)]^{1/2}$. So we are left with the task of solving the four linear equations for the unknown $t_2(k)$ as a function of the twelve calculated values for $a_{1,N-1}$, $b_{1,N-1}$, $c_{1,N-1}$, $a_{2,N-1}$, $b_{2,N-1}$, $c_{2,N-1}$, $a_{1,N}$, $b_{1,N}$, $c_{1,N}$, $a_{2,N}$, $b_{2,N}$ and $c_{2,N}$. We find as the final result the fraction

$$t_2(k) = [Z_1 \exp(-\kappa_u x_{N-1}) + Z_2 \exp(-\kappa_u x_N)] / [Z_3 \exp(-i k_d x_{N-1}) + Z_4 \exp(-i k_d x_N)] \quad (\text{B13})$$

where the four auxiliary parameters Z_i are given as

$$Z_1 = -a_{2,N-1} b_{2,N} c_{1,N} + a_{2,N} b_{2,N-1} c_{1,N} + a_{2,N-1} b_{1,N} c_{2,N} - a_{1,N} b_{2,N-1} c_{2,N} - a_{2,N} b_{1,N} c_{2,N-1} + a_{1,N} b_{2,N} c_{2,N-1} \quad (\text{B14a})$$

$$Z_2 = a_{2,N-1} b_{2,N} c_{1,N-1} - a_{2,N} b_{2,N-1} c_{1,N-1} - a_{2,N-1} b_{1,N-1} c_{2,N} + a_{1,N-1} b_{2,N-1} c_{2,N} + a_{2,N} b_{1,N-1} c_{2,N-1} - a_{1,N-1} b_{2,N} c_{2,N-1} \quad (\text{B14b})$$

$$Z_3 = (-b_{2,N} c_{1,N} + b_{1,N} c_{2,N}) \exp(-\kappa_u x_{N-1}) + (b_{2,N} c_{1,N-1} - b_{1,N-1} c_{2,N}) \exp(-\kappa_u x_N) \quad (\text{B14c})$$

$$Z_4 = (b_{2,N-1} c_{1,N} - b_{1,N} c_{2,N-1}) \exp(-\kappa_u x_{N-1}) + (-b_{2,N-1} c_{1,N-1} + b_{1,N-1} c_{2,N-1}) \exp(-\kappa_u x_N) \quad (\text{B14d})$$

References

- [1] For the Ultraphotonik – Polaris projects, see, <http://www.physik.uni-jena.de/inst/polaris>
- [2] For review of the Extreme Light Infrastructure (ELI) projects, see <http://www.extreme-light-infrastructure.eu/eli-home.php>
- [3] For review of the European X-Ray Laser Project XFEL, see <http://xfel.desy.de>
- [4] For a review, see, e.g., W. Greiner, B. Müller and J. Rafelski, “Quantum Electrodynamics of Strong Fields” (Springer Verlag, Berlin, 1985).
- [5] For a recent review, see, e.g., A. Di Piazza, C. Müller, K.Z. Hatsagortsyan and C.H. Keitel, *Rev. Mod. Phys.* 84, 1177 (2012).
- [6] H.K. Avetissian, “Relativistic Nonlinear Electrodynamics” (Springer, New York, 2006).
- [7] B.R. Holstein, *Am. J. Phys.* 66, 507 (1998)
- [8] B.R. Holstein, *Am. J. Phys.* 67, 499 (1999).
- [9] P. Krekora, Q. Su and R. Grobe, *Phys. Rev. Lett.* 92, 040406 (2004).
- [10] P. Krekora, K. Cooley, Q. Su and R. Grobe, *Phys. Rev. Lett.* 95, 070403 (2005).
- [11] J.S. Schwinger, *Phys. Rev.* 82, 664 (1951).
- [12] L.L. Foldy and S.A. Wouthuysen, *Phys. Rev.* 78, 29 (1950).
- [13] F. Hund, *Z. Phys.* 117, 1 (1941).
- [14] F. Fillion-Gourdeau, E. Lorin and A.D. Bandrauk, *Phys. Rev. Lett.* 110, 013002 (2013).
- [15] T. Cheng, M. Ware, Q. Su and R. Grobe, *Phys. Rev. A* 80, 062105 (2009).
- [16] V. Dinu, T. Heinzl, A. Ilderton, M. Marklund and G. Torgrimsson, *Phys. Rev. D* 89, 125003 (2014).
- [17] H. Gies and G. Torgrimsson, *Phys. Rev. Lett.* 116, 090406 (2016).
- [18] M. Yu. Kuchiev, *Phys. Rev. Lett.* 99, 130404 (2007).
- [19] S. Meuren, K.Z. Hatsagortsyan, C.H. Keitel and A. Di Piazza, *Phys. Rev. Lett.* 114, 143201 (2015).
- [20] For review, see T. Cheng, Q. Su and R. Grobe, *Contemp. Phys.* 51, 315 (2010).
- [21] A. Wachter, “Relativische Quantenmechanik” (Springer, Berlin, 2005).
- [22] J.W. Braun, Q. Su and R. Grobe, *Phys. Rev. A* 59, 604 (1999).
- [23] G.R. Mocken and C.H. Keitel, *Comp. Phys. Commun.* 178, 868 (2008).
- [24] M. Ruf, H. Bauke and C.H. Keitel, *J. Comp. Phys.* 228, 9092 (2009).
- [25] H. Bauke and C.H. Keitel, *Comp. Phys. Commun.* 182, 2454 (2011).
- [26] A.D. Bandrauk and H. Shen, *J. Phys. A* 27, 7147 (1994).

- [27] F. Sauter, *Z. Phys.* 69, 742 (1931).
- [28] F. Hebenstreit, J. Berges and D. Gelfand, *Phys. Rev. Lett.* 111, 201601 (2013).
- [29] F. Hebenstreit, J. Berges and D. Gelfand, *Phys. Rev. D* 87, 105006 (2013).
- [30] C.C. Gerry, Q. Su and R. Grobe, *Phys. Rev. A* 74, 044103 (2006).
- [31] G. R. Mocken, M. Ruf, C. Müller and C.H. Keitel. *Phys. Rev. A* 81, 022122 (2010).
- [32] F. Hebenstreit, R. Alkofer, and H. Gies, *Phys. Rev. D* 82, 105026 (2010).
- [33] R. Dabrowski and G. V. Dunne, *Phys. Rev. D* 90, 025021 (2014),
- [34] Q.Z. Lv, D.J. Jennings, J. Betke, Q. Su and R. Grobe, *Comp. Phys. Comm.* 198, 31 (2016).
- [35] P. Krekora, Q. Su and R. Grobe, *Phys. Rev. A* 73, 022114 (2006).